



Research Article

Application of the central composite design to mineralization of olive mill wastewater by the electro/Fell/persulfate oxidation method



Fatma Görmez¹ · Özkan Görmez¹  · Erdal Yabalak¹ · Belgin Gözmen¹

Received: 15 September 2019 / Accepted: 6 January 2020 / Published online: 10 January 2020
© Springer Nature Switzerland AG 2020

Abstract

The olive mill wastewater is a major environmental problem, which is waiting for effective treatment. In this study, the mineralization of olive mill wastewater was investigated using the electro/Fell/persulfate process. The central composite design was utilized to examine the effect of each experimental variables (concentration of persulphate and Fell, treatment time and constant current) on the mineralization of olive mill wastewater. The optimum chemical oxygen demand removal percentage was obtained as 71.2% where the reaction conditions were 200 mA current, 250 mM persulphate, 25 mM Fell, and 6 h reaction time. In addition, the maximum percentage of total phenolic removal and the energy consumption were 88% and 4.50 kWh/kgCOD, respectively, which were obtained at the same reaction conditions mentioned above. ANOVA test was used to examine the reliability of the experimental method. The R^2 and adjusted R^2 coefficients were obtained as 0.9634 and 0.9305, respectively. Optimum experimental parameters were determined and theoretical equations were obtained for the degradation of olive mill wastewater. For the treatment of olive mill wastewater, an environmentally friendly oxidation process was examined and the effect of each experimental variables was clearly demonstrated. The obtained data was optimized for future applications.

Keywords Advanced electro-oxidation processes · Mineralization · Olive mill wastewater · Persulfate · Response surface methodology

1 Introduction

The Olive oil industry is one of the most important economic resources of the world. Approximately 95–97% of olive oil produced worldwide is supplied by Mediterranean countries such as Spain, Italy, Greece and Turkey. While these countries earn a large income from the production of olive oil, this process produces wastes that cause considerable environmental problems. One of the most important problems of them is olive mill wastewater (OMW), which is produced as a subsequent about 40–120 L per ton during the production of olive oil [1–7].

Basically, the composition of olive mill wastewater may vary depending on the climate conditions, types of olive

trees, cultivation system, applied extraction methods and the structures of pesticides and fertilizers which are used for growing of olive fruit [8, 9]. Although the composition of OMW varies in a wide range, it is characterized by containing a high organic load, high chemical oxygen demand (COD) value (30–318 g/L), a high suspended solid content (24–120 g/L), representing low pH, plant toxicity, characteristic unpleasant odor and dark black-brown color properties [5, 9–11]. OMW's basic molecules such as phenolic compounds, tannins, organic acids, sugars, polysaccharides, proteins and lipids that form its organic matter content, are resistant to biodegradation [5, 12, 13].

OMW causes many undesired environmental problems such as blocking passage of the sun light by forming a

✉ Özkan Görmez, ozkan.grmz@gmail.com | ¹Department of Chemistry, Faculty of Arts and Science, Mersin University, 33343 Yenisehir, Mersin, Turkey.



colored layer on the surface of natural water, preventing oxygen transfer between water and atmosphere by forming an oily layer. In addition, it causes toxicity on the aquatic flora and living organisms, alterations in soil quality and gives off odor nuisance [9, 14–16].

Essentially, the toxic effect of OMW is mainly caused by a high content of phenolic compounds [17–19]. Although olive fruit is very rich in terms of phenolic compounds, only about 2% of it remains in olive oil phase during extractions. 98% of total phenolic compounds are released to the environment in OMW and olive pomace [20–22]. The amount of total phenolic contents in OMW varies from 1000 ppm up to 10,000 ppm [7]. In addition, phenolic compounds can polymerize to high molecular weight compounds, which are difficult to degrade by conventional methods, during storage [23, 24]. Thus, OMW, which is released into the environment without control in excessive amounts, poses a great risk to the environment.

Various processes such as aerobic biological treatment, anaerobic treatment method, electrochemical treatment, ultrafiltration, precipitation/flocculation, and evaporation ponds as well as a combined treatment process of these methods have been used in the treatment of OMW [5, 19, 25]. However, these methods do not provide high efficiency. Due to containing a lot of different resistant pollutants, researchers make efforts to improve new and more efficient methods for the degradation of OMW [5, 26, 27].

For example, in some Mediterranean countries, OMW wastewater is collected in evaporation ponds then used as soil amendment without any treatment. However, applying evaporation open ponds, a sludge is produced which is black, malodorous and hard to treat. Also, depending on the depth of the evaporation ponds, the area and seasonal conditions, the evaporation process time can be increased. The natural evaporation process also includes a natural biological treatment. The microbiological study for 5 evaporation ponds in Tunisia was shown that yeast and mold were dominant but the bacterial population decreased after 75 days. The pH value (in the range 4.5–5.8), high content of antibacterial and phytotoxic substances such as phenolic, fat and lipid of OMW prevents the growth of microorganisms and consequently it fails the biological treatment especially in the case of anaerobic digestion treatment. As a result, it is difficult to say that these methods leave the final products which are completely economical and harmless to the environment [28–30].

Recently, membrane methods that do not require the use of any chemicals and have less space need are noteworthy. Paraskeva et al. [31] treated OMW produced by the three-phase system using a pilot scale set-up consisting of ultrafiltration, nanofiltration, and reverse osmosis membranes. They turned 70% of the initial volume into water that could be emptied without risking the environment or

used for irrigation. However, the biggest disadvantage of membrane processes is higher first having investment and operating costs. Disposal of the concentrate solid waste after treatment is carried out by burning or sending to the landfill. Also, this method requires pre-filtration to prevent the membranes from becoming contaminated [31]. When the disadvantages of these methods are examined, it is clear that there is a need for powerful methods for the purification of OMW.

In recent years, electrochemical advanced oxidation processes (EAOPs), have attracted great attention due to their effectiveness in the degradation of toxic and persistent organic molecules in water. The interest in using these methods is due to features such as their environmental compatibility, versatility, presenting high efficiency in the removal of persistent organic molecules and offering operational safety. The other advantages of EAOPs are providing the operation facility in mild conditions and generating very powerful radicals in water which are essential in the degradation of target pollutants [32–34].

The electro/ Fe^{n+} /persulfate (E/Fe/PS) process, which is a combined process of metal ion and electro activation of persulfate, that favored the activation of persulfate, is an efficient degradation method of EAOPs, such as electro-Fenton (EF), photoelectro-Fenton (PEF) and electro-persulfate (EPS) [33, 35, 36]. Persulfate, which has high solubility, good stability, and high reactivity ($E^\circ = 2.1 \text{ V}$) is commonly used as an oxidizing agent. Persulfate is generally activated to produce sulfate free radicals ($\text{SO}_4^{\cdot-}$) which are capable for degradation of persistent pollutants. Persulfate turns into a sulphate molecule which is relatively harmless for the ecological functions of the environment at the end of the treatment process [34, 37]. Moreover, the accepted highest concentration of SO_4^{2-} ion in water is 250 ppm according to US EPA [38].

In the last few decades, many experimental design models have been used in experimental studies to reduce time and energy loss, as well as to show the effect of each experimental parameter and the interaction effects of them on the process. The response surface method (RSM) is one of the most important statistical methods which is used for the mentioned purpose by researchers. The central composite design (CCD) is a well-known second-order RSM model which is needed quite a few numbers of design points while providing a reasonable amount of information for testing lack of fit of the experimental model [39–45].

In this study, optimum working conditions of OMW treatment by the electro/Fe/PS oxidation method, based on both, transition metal and cathodic reduction of persulfate, were realized by applying the response surface method with the central composite design. Oxidation efficiency was measured by the COD removal, followed

by persulfate (PS) content and total phenolic (TP) removal percent at optimum conditions.

2 Experimental

2.1 Materials

Olive oil mill water, used for this study, was supplied from a local olive oil producing plant in Mersin. In this plant, Olive oil production is carried out using the traditional method. In the traditional method, olive oil is obtained by using hydraulic presses and hot water. The wastewater was allowed to cool to room temperature overnight. After centrifuged at 6000 rpm, samples were collected in polypropylene bottles, and kept at 4 °C, until further use. Characteristics of the OMW can be seen in Table 1. Potassium persulfate (K₂S₂O₈), iron (II) sulfate heptahydrate (FeSO₄·7H₂O), and chemical oxygen demand (COD) cell kits (0–15,000 mg/L) were purchased from Merck (Düsseldorf, Germany). Folin-Ciocalteu’s phenol reagent and Gallic acid (GA) were purchased from Sigma-Aldrich (St. Louis, MO). Anhydrous sodium carbonate was purchased from Fluka (USA). Ultra-pure water (18 MΩ cm at 25 °C) was provided using a Millipore Milli-Q Advantage A10.

2.2 Experimental design and optimization

The central composite design (CCD) was used for the response surface methodology in the experimental design. A CCD contains an imbedded factorial or fractional factorial design with center points which is augmented with a group of ‘star points’ that allow estimation of curvature. The CCD could be accepted the best design because of allowing the estimation of individual and interaction factor effects independently of the block effect which called orthogonal blocking [46]. The independent variables of the constant current (mA), PS concentration (mM),

Fell concentration (mM) were coded with low and high levels in the CCD design, as presented in Table 2. The COD and TP removal percents were chosen as the responses. Twenty experiments according to CCD matrix were performed for the degradation of OMW in the Electro/Fell/PS method as demonstrated in Table 3. The experimental results were analysed by Design Expert 9.0.6.2 version and the regression model was suggested.

The correlation of response and independent variables can be represented by linear or quadratic models (Eq. 1).

$$Y = \beta_0 + \beta_1x_1 + \beta_2x_2 + \beta_3x_3 + \beta_{12}x_1x_2 + \beta_{13}x_1x_3 + \beta_{23}x_2x_3 + \beta_{11}x_1^2 + \beta_{22}x_2^2 + \beta_{33}x_3^2 + \epsilon \tag{1}$$

where Y symbolizes the response and x₁, x₂ and x₃ depict the coded independent variable effects, and x₁², x₂² and x₃² represent the quadratic effects. x₁x₂, x₁x₃ and x₂x₃ demonstrate interaction effects. β₁, β₂, β₃ and β₁₁, β₂₂, β₃₃ represent the linear and quadratic coefficients, respectively. β₁₂, β₁₃ and β₂₃ are the interaction coefficients. β₀ and ε represent the constant and random error, respectively [47].

2.3 Experiments and sample analysis

In the experiments, 200 mL of 1:10 diluted OMW was used. The electro/Fell/PS experiments were carried out in a 250 mL of the cylindrical reactor made of glass material. An edge plane pyrolytic graphite (EPPG) (Momentive PG plate UEK, USA) electrode, which was prepared from the plates with a thickness of 0.5 cm (3 cm × 0.8 cm), was used as the cathode and a 10 cm² platinum gauze electrode was used as the anode. Fell and persulfate salts were added in the amounts determined according to the experimental design, and then electrolysis was performed in different constant current values. A Support electrolyte was not used as the wastewater conductivity was sufficient. The pH adjustment was not made and the treatment time was fixed at 360 min, which was determined according to the results of preliminary experiments. The anode and cathode sets were connected to the positive and negative outlets of a DC power source (NEL PS2000 DC) with a maximum

Table 1 The content of OMW

Parameters	Value	
	Raw OMW	Diluted (1:10) OMW
pH	5.01 ± 0.03	5.06 ± 0.05
Conductivity (ms/cm)	6.38 ± 0.07	0.81 ± 0.04
Total solids (g/L)	24.00 ± 0.61	Nm
Ash (g/L)	6.20 ± 0.18	Nm
Soluble total phenolic (mg/L)	nm	1887.00 ± 11.02
Soluble COD (mg/L)	nm	6265.00 ± 6.56
Soluble absorbance at UV ₂₅₄	nm	17.45 ± 1.15

nm not measured

Table 2 Experimental range and levels of the independent variables for degradation of OMW by the electro/Fell/PS method

Factors: independent variables name	Coded levels				
	-α	-1	0	+1	+α
x ₁ : PS concentration (mM)	44.87	100	175	250	301.13
x ₂ : Fell concentration (mM)	3.18	10	20	30	36.82
x ₃ : Constant current (mA)	132	200	300	400	468

Table 3 Central composite design for oxidation of OMW and observed response of the COD removal %, and residue PS

Run	Actual (coded) levels			COD removal, %		Residue PS (mM)
	PS concentration (mM)	Fe concentration (mM)	Constant current (mA)	Exp.	Pre.	
1	100 (-1)	10 (-1)	200 (-1)	40.47	38.45	1.194
2	175 (0)	20 (0)	300 (0)	59.74	55.35	1.766
3	175 (0)	20 (0)	468 (+1.682)	60.64	62.32	1.877
4	100 (-1)	30 (+1)	400 (+1)	43.13	42.60	2.682
5	175 (0)	36.82 (+1.682)	300 (0)	52.30	49.46	2.254
6	301.13 (+1.682)	20 (0)	300 (0)	80.00	78.86	6.092
7	175 (0)	20 (0)	300 (0)	53.19	55.35	1.755
8	175 (0)	20 (0)	132 (-1.682)	60.96	59.90	1.877
9	250 (+1)	30 (+1)	400 (+1)	68.68	70.27	2.729
10	100 (-1)	30 (+1)	200 (-1)	40.15	41.67	2.574
11	175 (0)	20 (0)	300 (0)	57.78	55.35	1.774
12	250 (+1)	10 (-1)	400 (+1)	64.51	62.56	9.880
13	48.87 (-1.682)	20 (0)	300 (0)	35.20	36.96	1.960
14	175 (0)	20 (0)	300 (0)	50.93	55.35	2.134
15	175 (0)	20 (0)	300 (0)	55.02	55.35	1.745
16	175 (0)	3.18 (-1.682)	300 (0)	36.82	40.27	2.022
17	100 (-1)	10 (-1)	400 (+1)	48.06	45.78	1.272
18	250 (+1)	10 (-1)	200 (-1)	60.52	60.61	0.840
19	250 (+1)	30 (+1)	200 (-1)	72.87	74.72	2.612
20	175 (0)	20 (0)	300 (0)	55.53	55.35	1.872

Experimental Exp., Predicted Pre

current rating of 3 A. The samples were filtered through NY-0.45 µm syringe filters.

A total phenolic content was estimated based on Folin–Ciocalteu method and the calibration curve was prepared from 25 to 800 mg/L by selecting gallic acid as standard [48]. Briefly, 1 mL of Folin–Ciocalteu reagent and 1 mL of sample solution are mixed. Then, the mixture was held in dark for 5 min. Next, 2 mL of Na₂CO₃ solution (20% w/v) and 2 mL of distilled water are added to this mixture and resulting mixture was stored in the dark for 30 min. Finally, the absorbance of the mixture was recorded the spectrometer (Shimadzu, Japan) at a wavelength of 714 nm.

The total phenolic removal percent was calculated through the equation below

$$TP \text{ Removal\%} = \frac{TP_i - TP_t}{TP_i} \times 100 \quad (2)$$

where TP_i and TP_t refer to the TP content of the initial and treated sample, respectively.

Before the COD measurement, the Fe ions in the medium were precipitated by raising the pH. In addition, PS would interfere with COD measurements, the PS value was estimated in samples and COD value was corrected

as mentioned in a previous study [36]. The Persulfate content of treated aqueous samples was analyzed spectrometrically according to the method mentioned below at the end of the treatment time. Briefly, 0.2 g of NaHCO₃ and 4 g of KI were solved into 40 mL water. A 100 µL of sample was added to this mixture and the mixture was shaken and allowed to equilibrate for 15 min in the dark [49]. The calibration graph was linear in the range of persulfate solution concentration of 0–50 mM at 352 nm by UV–Vis (Shimadzu). The COD measurements were monitored by the COD cell kit, which can function between 0 and 15,000 mg/L of value. A Spectroquant NOVA 30 photometer was used to monitor COD values of treated and untreated samples.

3 Results and discussion

3.1 Evaluation of the obtained model by ANOVA

The effects of the variables on the COD removal percentage in the electro/FeII/PS oxidation of 1:10 diluted OMW were investigated with RSM using CCD. The obtained COD removal percentage, residual PS amount and TP removal

percentage were given in Table 3. The results of the COD removal percentage were fitted to the quadratic model with the R^2 value of 0.9634 when the matrix was arranged according to the CCD. In the conducted study, the percentage of COD removal from wastewater with an initial COD content of 6265 mg/L varied between 35.2 and 80.0%.

ANOVA of CCD model was evaluated to prove the model fitting of the experimental data. Table 4 shows the ANOVA results of the quadratic model for the COD removal percentage of OMW. It can be seen that the proposed model was highly significant depending on very low p values (< 0.0001). The fact that the F value of the obtained model (29.28) was higher than the tabulated F value ($F_{0.05, df, (n-(df+1))} = 3.02$) of the table is a proof of the model fit. The other indicators of the model fit were high values of R^2 and adjusted R^2 coefficients, which were obtained as 0.9634 and 0.9305, respectively.

3.2 Multiple regression modeling

The obtained experimental data shown in Table 3 were used to fit the polynomial model representing the COD removal% (response, Y) as a function of both PS and Fe initial concentration and applied current and fit model equation was shown below (Eq. 3):

$$Y = 12.46x_1 + 2.73x_2 + 0.72x_3 + 2.72x_1x_2 - 1.35x_1x_3 - 1.60x_2x_3 + 0.90x_1^2 - 3.71x_2^2 + 2.04x_3^2 + 55.35 \tag{3}$$

Model coefficients with standard deviation were also given in the Table 4. Pareto graph analysis, which introduces the positive or negative single, quadratic or interactive effect of the variables on the COD removal efficiency was given in Fig. 1 [50, 51].

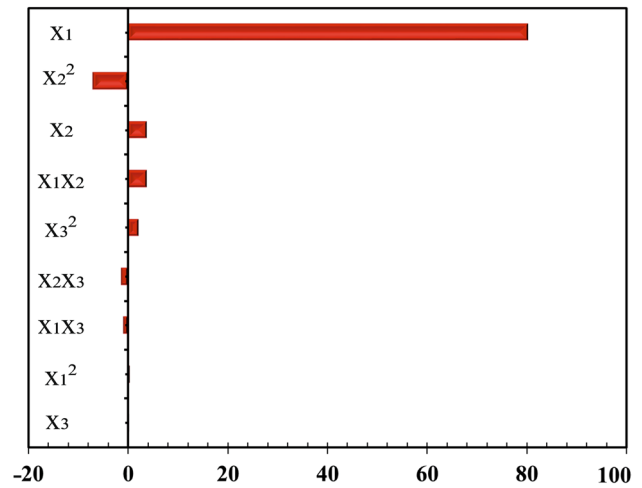


Fig. 1 Graphical Pareto chart

It is clear that the most effective parameter for the COD removal of OMW was x_1 . However, it is observed that the linear effect of x_1 is more than quadratic effect (x_1^2) of it. In other words, the increase of the PS concentration increases the COD removal linearly. While Fell concentration (x_2) was the second positive effective parameter, applied current amount (x_3) was a very inef-

fective parameter on the COD removal of the OMW. The quadratic effect (x_2^2) of the variable x_2 is greater than linear effect of it. At first, the increase in the Fell concentration first increased the COD removal efficiency, but

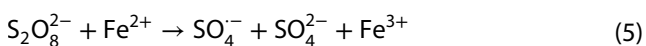
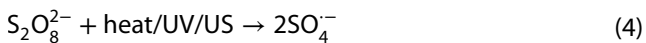
Table 4 ANOVA results and coefficients of the quadratic models for COD removal percentage obtained by CCD

Source	COD removal %				Coefficient estimate (β)
	Mean square	df	F Value	p value prob > F	
Model	2620.52	9	29.28	<0.0001	55.35 (± 1.29)
x_1	2119.00	1	213.07	<0.0001	12.46 (± 0.85)
x_2	101.90	1	10.25	0.0095	2.73 (± 0.85)
x_3	7.08	1	0.71	0.4186	0.72 (± 0.85)
x_1x_2	59.24	1	5.96	0.0348	2.72 (± 1.11)
x_1x_3	14.50	1	1.46	0.2550	-1.35 (± 1.11)
x_2x_3	20.45	1	2.06	0.1821	-1.60 (± 1.11)
x_1^2	11.79	1	1.19	0.3017	0.90 (± 0.83)
x_2^2	197.90	1	19.90	0.0012	-3.71 (± 0.83)
x_3^2	59.74	1	6.01	0.0342	2.04 (± 0.83)
Residual	99.45	10			
Lack of Fit	49.93	5	1.01	0.4965	
Pure error	49.52	5			
Total	2719.97	19			

then caused the decline. In addition, variables x_1 and x_2 showed synergistic effects (x_1x_2) for the COD removal.

3.3 Three-dimensional (3D) response surfaces

$SO_4^{\cdot-}$ radical is more aggressive than persulfate and can degrade pollutants more effectively. Persulfate can be activated in various reactions based on using heat, base, H_2O_2 , UV, ultrasound (US), transition metals or cathodic reduction to produce $SO_4^{\cdot-}$ radical as shown in the following reactions [34, 37, 52–54].



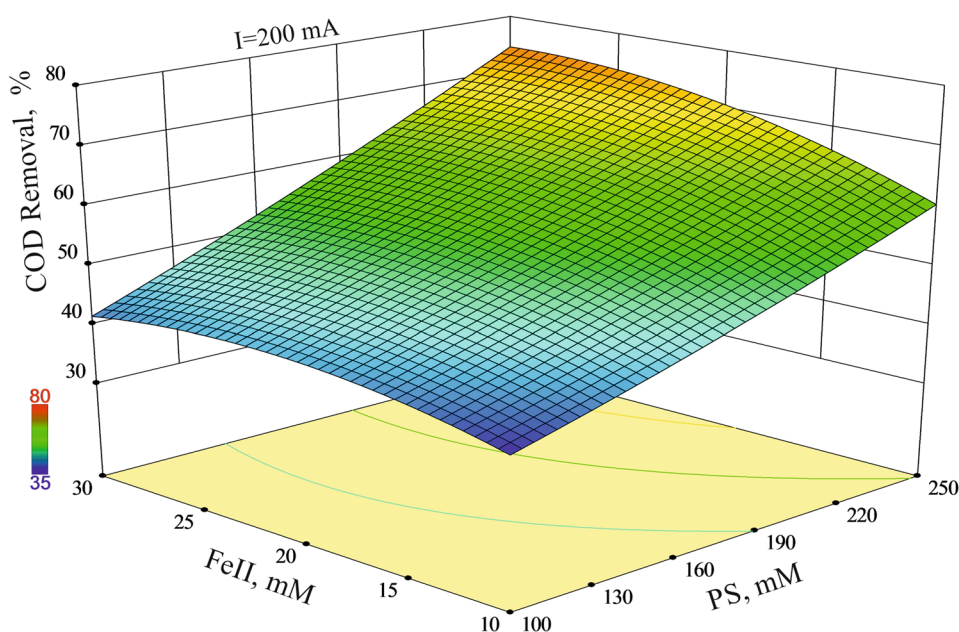
As known, $\cdot OH$ is a very powerful and non-selective oxidant which is used for removing of persistent organic pollutants. When the redox potentials of $SO_4^{\cdot-}$ ($E^0 = 2.6\text{ V}$) and $\cdot OH$ ($E^0 = 2.7\text{ V}$) are compared, it is seen that the redox potentials of them are very close [37, 55]. However, there are several prominent features that make it possible to prefer sulphate radical to $\cdot OH$ radicals. The first advantage of using $SO_4^{\cdot-}$ is providing working at acidic pH levels. Secondly, sulphate radical is more stable in water and the lifetime of $SO_4^{\cdot-}$ (30–40 μs) is longer than the $\cdot OH$ ones (20 ns). In addition to these properties, the sulphate radicals have high solubility and offer an effective working chance on a wide pH range [56].

For the production of sulphate radical, iron can be used as a metal source, which is relatively harmless and quite cheap. Iron provides the activation of persulfate to sulphate radicals by requiring lower activation energy according to thermal activation. However, it must not be forgotten that the excess of iron can cause undesirable results during the production of radicals. Excess ferrous ions can enter the reaction with radicals and cause them to be damped. Thus, the optimised amount of iron must be used in oxidation reactions [37, 57].

In the control studies, only 9.7% COD removal was obtained after 6 h of electro-PS treatment with 100 mM PS in the absence of ferrous ion (Eq. 6). When the wastewater, containing 20 mM Fe and 200 mM PS, was kept for 6 h at ambient conditions, a COD removal of 15% was achieved (Eq. 5). In the previous study, it was elaborated in detail that the electro-PS and metal catalysed-PS oxidation methods alone were not effective [33].

The 3D graphs, providing valuable insight on the influences of the independent variables and their interactions on the dependent variables, were obtained based on Eq. 6. The interactive effect of PS concentration and Fe^{II} concentration on the COD removal percentage while holding current at 200 mA was shown in Fig. 2. As mentioned earlier, the initial concentration of PS was the most effective variable on COD removal of OMW. Therefore, a linear increase in the COD removal, due to the increase in PS concentration, was observed. At the same time, it is seen that this increase in the COD elimination is also influenced by the amount of Fe^{II} . In other words, the synergistic effect of the two variables was arisen. With Fe^{II} concentrations of 10 and 25 mM, the COD removal increased by 57% and 70%,

Fig. 2 Interactive effect of initial concentrations of Fe^{II} and PS on the COD removal percentage of OMW



respectively, when the PS concentration was increased from 100 to 250 mM.

Figure 3 presents the interactive effect of PS concentration and applied current amount at constant initial FeII concentration (25 mM). The applied current amount was found as the most ineffective variable on COD removal, as seen from the Pareto chart graph (Fig. 1). It is more appropriate to work at low currents because of the high cost at high current values.

The interactive effect of FeII concentration and applied current amount at constant initial PS concentration

(250 mM) was given in Fig. 4. FeII concentration is another variable that is effective on the COD removal. Figure 4 shows that the COD removal increased from 61% to 71% when the FeII concentration was increased from 10 mM to 20 mM. However, this efficiency slowed down above this concentration. For example, the results obtained for 25 and 30 mM were 73% and 75%, respectively.

Fig. 3 Interactive effect of PS concentration and applied current on the COD removal percentage of OMW

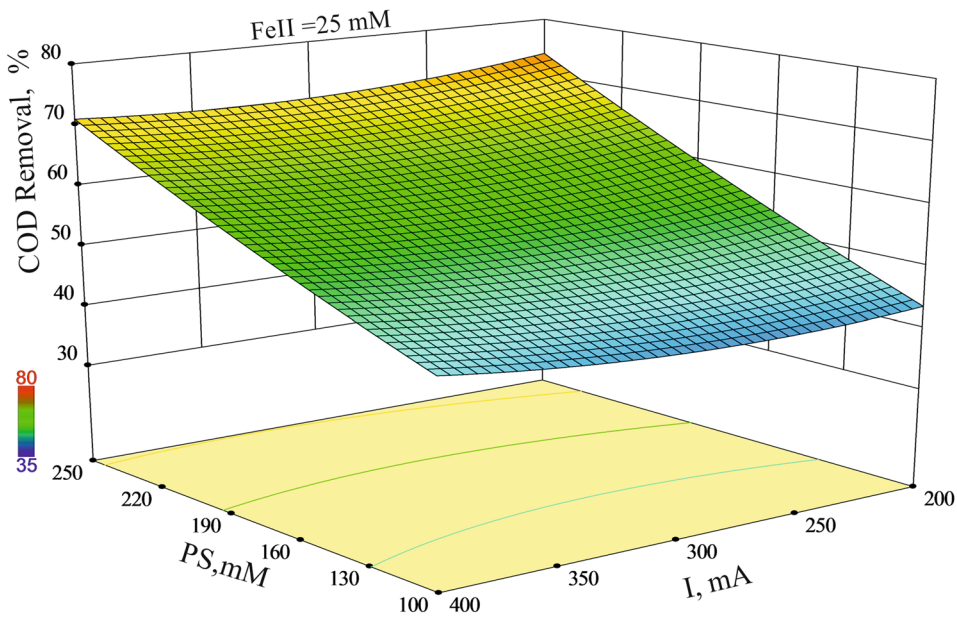
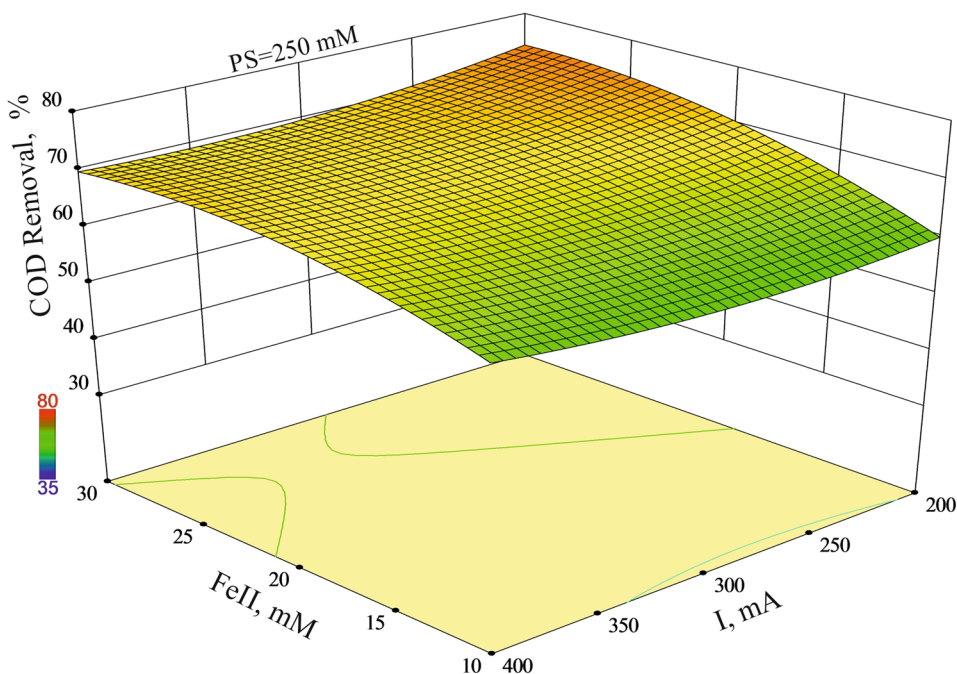


Fig. 4 Interactive effect of FeII concentration and applied current on the percentage of COD removal of OMW



3.4 The optimization

Optimum condition and a condition close to the optimum value, which were within the CCD range, were set for maximum COD removal and validation experiments were performed on these conditions (Table 5). It was observed that the percentage of obtained COD removal and the predicted values of the model were in harmony with each other for 6 h of treatment time. In both cases, approximately 50–60% COD removal was achieved for the first 3 h, but the degradation rate slowed in the following time. When the PS residue concentration was examined, 27–29 mM of PS were determined after 3 h. In case of increased electrolysis time, the concentration of PS decreased which could indicate that sufficient radical production ensured. In case of TP removal in OMW, when 200 mM of PS, 200 mA of current, and 25 mM of FeII were applied, the obtained efficiency achieved after 3 and 6 h was 61% and 88%, respectively.

Moreover, the energy consumption at the optimum conditions after 6 h treatment (Table 5) was calculated as follows [58]:

$$\text{Energy consumption (kWh (kgCOD)}^{-1}) = \frac{Ivt}{(\Delta\text{COD})V_s} \quad (7)$$

where *I* is the applied current (A), *V* is the average cell voltage (V), *t* is electrolysis time (h), *V_s* is the solution volume (L), and ΔCOD is the decay in COD (g/L).

According to the results in Table 5, when we compare the energy consumption in our study with the values of similar studies in the literature, our results seem quite good. For example, Barbosa et al., obtained 44.6% COD removal efficiency after 7 h of electrooxidation of diluted OMW (1:3, 5188 mg/L initial COD concentration) using BDD anode, and calculated energy consumption as 42 kWh/kgCOD [59]. Also, Gotsi et al. has performed electrooxidation of OMW using stainless steel 316 L cathode and titanium (Grade II/VII) anode (covered by a thin film of tantalum, platinum and iridium alloy) and reached 27.1 kWh/kgCOD energy consumption with low COD removal after 120 min [60].

Some of the electrochemical methods previously applied for OMW treatment were given in Table 6. Compared with the methods in the table, the electro/Fe/PS method may require more chemicals, but it can be said that it is more effective at lower current values and shorter treatment time.

4 Conclusion

The treatment of OMW was investigated by the electro/FeII/Persulfate process using response surface methodology. The influence of applied current and the initial concentration of PS and FeII ions on the removal efficiencies of COD and TP was analysed. The electrochemical treatment

Table 5 The validation experiments for OMW treatment by the electro/FeII/PS system

Conditions			COD Removal %		Time (h)	PS residue (mM)	TP Removal %	Energy Consumption (kWh/kgCOD)
I (mA)	[PS] ₀ (mM)	[FeII] ₀ (mM)	Actual	Predicted				
200	250	25	59.4	74.0 ± 3.2	3	29.2	61	5.40
			66.2		5	5.02	69	4.84
			71.2		6	4.84	88	4.50
200	200	20	46.7	61.4 ± 3.2	3	27.4	48	7.64
			53.5		5	3.99	61	6.67
			63.4		6	2.01	73	5.63

Table 6 Electrochemical processes of OMW

Method	Initial COD, g/L	Conditions	COD removal %	References
Electro-oxidation	65	platinized Ti-N electrodes separated by a cationic exchange membrane, V = 500 mL, t = 10 h, j = 3.5 A/dm ²	55	[61]
Anodic-oxidation	10	BDD anode, I = 30 A, t = 14 h	73	[62]
Anodic-oxidation	5.19	Si/BDD anode, j = 30 mA/cm ² , 7 h	44.6	[59]
Electro-oxidation	15.5	3% NaCl as the electrolyte, t = 8 h, V = 16 V	70	[63]
Electro-Fenton	1.840	V = 100 mL, t = 7 h, I = 200 mA, pH = 3, Carbon felt cathode, Pt anode, Fe ²⁺ = 0.1 mM	90	[64]
Active chlorine	26.75	Ti/TiRuO ₂ anode, stainless steel cathode, I = 5 A; NaCl = 5 g/L, t = 17 h	Almost complete	[65]

of OMW was optimized by using the CCD method. The reliability of the method was proved by the R^2 and adjusted R^2 values which were obtained as 0.9634 and 0.9305, respectively. The optimum COD and TP removal efficiencies were obtained as 71.2% and 88% at 6 h of treatment time, 200 mA current, 250 mM PS, and 25 mM Fell initial concentration. Also, the maximum and minimum value of TOC removal rate was obtained as 35.2% and 80.0%. The energy consumption at optimum condition was calculated as 4.50 kWh/kg COD for 6 h of electrolysis. Additionally, it is possible to increase the efficiency by increasing the PS concentration and the reaction time through considering economic and environmental sensitivities.

OMW cannot be treated directly by a single method because of its complex and intense organic pollutant content as cited in many studies in the literature. However, the results obtained in our study show that the electro/Fell/Persulfate process can be used effectively with combined other advanced oxidation methods for the treatment of real olive mill wastewater.

Acknowledgements This work was funded by Mersin University Research Fund (Project No: BAP 2017-1-AP3-2243). This academic work was linguistically supported by the Mersin Technology Transfer Office Academic Writing Center of Mersin University.

Compliance with ethical standards

Conflict of interest On behalf of all authors, the corresponding author states that there is no conflict of interest.

References

- Bravo KAS, Lopez FNA, Garcia PG, Quintana MCD, Fernandez AG (2007) Treatment of green table olive solutions with ozone. Effect on their polyphenol content and on *Lactobacillus pentosus* and *Saccharomyces cerevisiae* growth. *Int J Food Microbiol* 114:60–68. <https://doi.org/10.1016/j.ijfoodmicro.2006.09.032>
- El-Abbassi A, Saadaoui N, Kiai H, Raiti J, Hafidi A (2017) Potential applications of olive mill wastewater as biopesticide for crops protection. *Sci Total Environ* 576:10–21. <https://doi.org/10.1016/j.scitotenv.2016.10.032>
- Hanafi F, Belaoufi A, Mountadar M, Assobhei O (2011) Augmentation of biodegradability of olive mill wastewater by electrochemical pre-treatment: effect on phytotoxicity and operating cost. *J Hazard Mater* 190:94–99. <https://doi.org/10.1016/j.jhazmat.2011.02.087>
- Katsoni A, Frontistis Z, Xekoukoulotakis NP, Diamadopoulos E, Mantzavinos D (2008) Wet air oxidation of table olive processing wastewater: determination of key operating parameters by factorial design. *Water Res* 42:3591–3600. <https://doi.org/10.1016/j.watres.2008.05.007>
- Mert BK, Yonar T, Kiliç MY, Kestioğlu K (2010) Pre-treatment studies on olive oil mill effluent using physicochemical, Fenton and Fenton-like oxidations processes. *J Hazard Mater* 174:122–128. <https://doi.org/10.1016/j.jhazmat.2009.09.025>
- Yay ASE, Oral HV, Onay TT, Yenigün O (2012) A study on olive oil mill wastewater management in Turkey: a questionnaire and experimental approach. *Resour Conserv Recycl* 60:64–71. <https://doi.org/10.1016/j.resconrec.2011.11.009>
- Yabalak E, Görmez Ö, Gözmen Sönmez B (2018) Degradation, dephenolisation and dearomatisation of olive mill wastewater by subcritical water oxidation method using hydrogen peroxide: application of multi-response central composite design. *J Serb Chem Soc* 83:489–502. <https://doi.org/10.2298/JSC170909113Y>
- Kallel M, Belaid C, Mechichi T, Ksibi M, Elleuch B (2009) Removal of organic load and phenolic compounds from olive mill wastewater by Fenton oxidation with zero-valent iron. *Chem Eng J* 150:391–395. <https://doi.org/10.1016/j.cej.2009.01.017>
- Ioannou-Ttfofa L, Micheal-Kordatou I, Fattas FT, Eusebio A, Ribeiro B, Rusan M, Amer ARB, Zuraiqi S, Waismand M, Linder C, Wiesman Z, Gilron J, Fatta-Kassinos D (2017) Treatment efficiency and economic feasibility of biological oxidation, membrane filtration and separation processes, and advanced oxidation for the purification and valorization of olive mill wastewater. *Water Res* 114:1–13. <https://doi.org/10.1016/j.watres.2017.02.020>
- Amor C, Lucas MS, García J, Dominguez JR, De Heredia JB, Peres JA (2015) Combined treatment of olive mill wastewater by Fenton's reagent and anaerobic biological process. *J Environ Sci Health A* 50:161–168. <https://doi.org/10.1080/10934529.2015.975065>
- Yalılı Kılıç M, Yonar T, Kestioğlu K (2013) Pilot-scale treatment of olive oil mill wastewater by physicochemical and advanced oxidation processes. *Environ Technol* 34:1521–1531. <https://doi.org/10.1080/09593330.2012.758663>
- Andreozzi R, Longo G, Majone M, Modesti G (1998) Integrated treatment of olive oil mill effluents (OME): study of ozonation coupled with anaerobic digestion. *Water Res* 32:2357–2364. [https://doi.org/10.1016/S0043-1354\(97\)00440-5](https://doi.org/10.1016/S0043-1354(97)00440-5)
- Turano E, Curcio S, Paola M, Calabro V, Iorio G (2002) An integrated centrifugation-ultrafiltration system in the treatment of olive mill wastewater. *J Membr Sci* 209:519–531. [https://doi.org/10.1016/S0376-7388\(02\)00369-1](https://doi.org/10.1016/S0376-7388(02)00369-1)
- Canizares P, Lobato J, Paz R, Rodrigo MA, Saez C (2007) Advanced oxidation processes for the treatment of olive-oil mills wastewater. *Chemosphere* 67:832–838. <https://doi.org/10.1016/j.chemosphere.2006.10.064>
- Kestioğlu K, Yonar T, Azbar N (2005) Feasibility of physicochemical treatment and advanced oxidation processes (AOPS) as a means of pre-treatment olive mill effluent (OME). *Process Biochem* 40:2409–2416. <https://doi.org/10.1016/j.procbio.2004.09.015>
- Ochando-Pulido JM, Pimentel-Moral S, Verardo V, Martinez-Ferez A (2017) A focus on advanced physico-chemical processes for olive mill wastewater treatment. *Sep Purif Technol* 179:161–174. <https://doi.org/10.1016/j.seppur.2017.02.004>
- Azabou S, Najjar W, Gargoubi A, Ghorbel A, Sayadi S (2007) Catalytic wet peroxide photo-oxidation of phenolic olive oil mill wastewater contaminants part II. Degradation and detoxification of low-molecular mass phenolic compounds in model and real effluent. *Appl Catal B* 77:166–174. <https://doi.org/10.1016/j.apcatb.2007.07.008>
- D'Antuono I, Kontogianni VG, Kotsiou K, Linsalata V, Logrieco AF, Tasioula-Margari M, Cardinali A (2014) Polyphenolic characterization of olive mill wastewaters, coming from Italian and Greek olive cultivars, after membrane technology. *Food Res Int* 65:301–310. <https://doi.org/10.1016/j.foodres.2014.09.033>
- Garcia CA, Hodaifa G (2017) Real olive oil mill wastewater treatment by photo Fenton system using artificial ultraviolet light lamps. *J Clean Prod* 162:743–753. <https://doi.org/10.1016/j.jclepro.2017.06.088>
- Poerschmann J, Baskyr I, Weiner B, Koehler R, Wedwitschka H, Kopinke FD (2013) Hydrothermal carbonization of olive

- mill wastewater. *Bioresour Technol* 133:581–588. <https://doi.org/10.1016/j.biortech.2013.01.154>
21. Rodis PS, Karathanos VT, Mantzavinou A (2002) Partitioning of olive oil antioxidants between oil and water phases. *J Agric Food Chem* 50:596–601. <https://doi.org/10.1021/jf010864j>
 22. La Scalia G, Micale R, Cannizzaro L, Marra FP (2017) A sustainable phenolic compound extraction system from olive oil mill wastewater. *J Clean Prod* 142:3782–3788. <https://doi.org/10.1016/j.jclepro.2016.10.086>
 23. Crognale S, D'Annibale A, Federici F, Fenice M, Quarantino D, Petruccioli M (2006) Olive oil mill wastewater valorisation by fungi. *J Chem Technol Biotechnol* 81:1547–1555. <https://doi.org/10.1002/jctb.1564>
 24. Gonçalves C, Lopes M, Ferreira JP, Belo I (2009) Biological treatment of olive mill wastewater by non-conventional yeasts. *Bioresour Technol* 100:3759–3763. <https://doi.org/10.1016/j.biortech.2009.01.004>
 25. Koutsos TM, Chatzistathis T, Balampekou EI (2018) A new framework proposal, towards a common EU agricultural policy, with the best sustainable practices for the re-use of olive mill wastewater. *Sci Total Environ* 622–623:942–953. <https://doi.org/10.1016/j.scitotenv.2017.12.073>
 26. Aytar P, Gedikli S, Sam M, Farizoğlu B, Çabuk A (2013) Sequential treatment of olive oil mill wastewater with adsorption and biological and photo-Fenton oxidation. *Environ Sci Pollut Res* 20(5):3060–3067. <https://doi.org/10.1007/s11356-012-1212-6>
 27. Doğruel S, Olmez-Hanci T, Kartal Z, Arslan-Alaton I, Orhon D (2009) Effect of Fenton oxidation on the particle size distribution of organic carbon in olive mill wastewater. *Water Res* 43:3974–3983. <https://doi.org/10.1016/j.watres.2009.06.017>
 28. Esfandyari Y, Mahdavi Y, Seyedsalehi M, Hoseini M, Safari GH, Ghozikali MG, Kamani H, Jaafari J (2015) Degradation and biodegradability improvement of the olive mill wastewater by peroxi-electrocoagulation/electrooxidation-electroflotation process with bipolar aluminum electrodes. *Environ Sci Pollut Res* 22:6288–6297. <https://doi.org/10.1007/s11356-014-3832-5>
 29. Jarbouli R, Hadrich B, Gharsallah N, Ammar E (2009) Olive mill wastewater disposal in evaporation ponds in Sfax (Tunisia): moisture content effect on microbiological and physical chemical parameters. *Biodegradation* 20:845–858. <https://doi.org/10.1007/s10532-009-9272-0>
 30. Tsioulpas A, Dimou D, Iconomou D, Aggelis G (2002) Phenolic removal in olive oil mill wastewater by strains of *Pleurotus* spp. in respect to their phenol oxidase (laccase) activity. *Bioresour Technol* 84:251–257. [https://doi.org/10.1016/S0960-8524\(02\)00043-3](https://doi.org/10.1016/S0960-8524(02)00043-3)
 31. Paraskeva CA, Papadakis VG, Tsarouchi E, Kanellopoulou DG, Koutsoukos PG (2007) Membrane processing for olive mill wastewater fractionation. *Desalination* 213:218–229. <https://doi.org/10.1016/j.desal.2006.04.087>
 32. Almeida LC, Garcia-Segura S, Arias C, Bocchi N, Brillas E (2012) Electrochemical mineralization of the azo dye Acid Red 29 (Chromotrope 2R) by photoelectro-Fenton process. *Chemosphere* 89:751–758. <https://doi.org/10.1016/j.chemosphere.2012.07.007>
 33. Gozmen B, Sonmez O, Sozutek A (2018) Comparative mineralization of basic red 18 with electrochemical advanced oxidation processes. *J Serb Chem Soc* 83(1):93–105. <https://doi.org/10.2298/JSC170227095G>
 34. Tsitonaki A, Petri B, Crimi M, Mosbaek H, Siegrist RL, Bjerg PL (2010) In situ chemical oxidation of contaminated soil and groundwater using persulfate: a review. *Crit Rev Environ Sci Technol* 40:55–91. <https://doi.org/10.1080/10643380802039303>
 35. Long A, Zhang H (2015) Selective oxidative degradation of toluene for the recovery of surfactant by an electro/Fe²⁺/persulfate process. *Environ Sci Pollut Res* 22:11606–11616. <https://doi.org/10.1007/s11356-015-4406-x>
 36. Zhang H, Wang Z, Liu C, Guo Y, Shan N, Meng C, Sun L (2014) Removal of COD from landfill leachate by an electro/Fe²⁺/persulfate process. *Chem Eng J* 250:76–82. <https://doi.org/10.1016/j.cej.2014.03.114>
 37. Vicente F, Santos A, Romero A, Rodriguez S (2011) Kinetic study of diuron oxidation and mineralization by persulfate: effects of temperature, oxidant concentration and iron dosage method. *Chem Eng J* 170:127–135. <https://doi.org/10.1016/j.cej.2011.03.042>
 38. Lau TK, Chu W, Graham NJD (2007) The aqueous degradation of butylated hydroxyanisole by UV/S₂O₈²⁻: study of reaction mechanisms via dimerization and mineralization. *Environ Sci Technol* 41:613–619. <https://doi.org/10.1021/es061395a>
 39. Aghaeinejad-Meybodi A, Ebadi A, Shafiei S, Khataee AR, Kiadehi AD (2019) Degradation of fluoxetine using catalytic ozonation in aqueous media in the presence of nano-γ-alumina catalyst: experimental, modeling and optimization study. *Sep Purif Technol* 211:551–563. <https://doi.org/10.1016/j.seppur.2018.10.020>
 40. Izadiyan P, Hemmateenejad B (2016) Multi-response optimization of factors affecting ultrasonic assisted extraction from Iranian basil using central composite design. *Food Chem* 190:864–870. <https://doi.org/10.1016/j.foodchem.2015.06.036>
 41. Ding H, Zhao D, Gao Y (2017) Response surface optimization of cholesterol extraction from lanolin alcohol by selective solvent crystallization. *Chem Pap* 71:71–79. <https://doi.org/10.1007/s11696-016-0043-1>
 42. Kalderis D, Kayan B, Akay S, Kulaksiz E, Gozmen B (2017) Adsorption of 2,4-dichlorophenol on paper sludge/wheat husk biochar: process optimization and comparison with biochars prepared from wood chips, sewage sludge and hog fuel/demolition waste. *J Environ Chem Eng* 5(3):2222–2231. <https://doi.org/10.1016/j.jece.2017.04.039>
 43. Sakkas VA, Islam MA, Stalikas C, Albanis TA (2010) Photocatalytic degradation using design of experiments: a review and example of the Congo red degradation. *J Hazard Mater* 175:33–44. <https://doi.org/10.1016/j.jhazmat.2009.10.050>
 44. Yabalak E, Gormez O, Gizir AM (2018) Subcritical water oxidation of prophan by H₂O₂ using response surface methodology (RSM). *J Environ Sci Health Part B Pesticides Food Contam Agric Wastes* 53(5):334–339. <https://doi.org/10.1080/03601234.2018.1431468>
 45. Oz Aksoy D, Sagol E (2016) Application of central composite design method to coal flotation: modelling, optimization and verification. *Fuel* 183:609–616. <https://doi.org/10.1016/j.fuel.2016.06.111>
 46. NIST/SEMATECH (2012) e-Handbook of statistical methods. <http://www.itl.nist.gov/div898/handbook/>
 47. Zhang Z, Zheng H (2009) Optimization for decolorization of azo dye acid green by ultrasound and H₂O₂ using response surface methodology. *J Hazard Mater* 172:1388–1393. <https://doi.org/10.1016/j.jhazmat.2009.07.146>
 48. Box JD (1983) Investigation of the Folin–Ciocalteu phenol reagent for the determination of polyphenolic substance in natural waters. *Water Res* 17:511–525. [https://doi.org/10.1016/0043-1354\(83\)90111-2](https://doi.org/10.1016/0043-1354(83)90111-2)
 49. Liang C, Huang C-F, Mohanty N, Kurakalva RM (2008) A rapid spectrophotometric determination of persulfate anion in ISCO. *Chemosphere* 73:1540–1543. <https://doi.org/10.1016/j.chemosphere.2008.08.043>
 50. Hammami S, Oturan N, Bellakhal N, Dachraoui M, Oturan MA (2007) Oxidative degradation of direct orange 61 by electro-Fenton process using a carbon felt electrode: application of the experimental design methodology. *J Electroanal Chem* 610:75–84. <https://doi.org/10.1016/j.jelechem.2007.07.004>

51. Gozmen B, Sonmez O, Turabik M (2013) Response surface methodology for oxidative degradation of the basic yellow 28 dye by temperature and ferrous ion activated persulfate. *Asian J Chem* 25:6831–6839. <https://doi.org/10.14233/ajchem.2013.14941>
52. Lin H, Wu J, Zhang H (2013) Degradation of bisphenol A in aqueous solution by a novel electro/Fe³⁺/peroxydisulfate process. *Sep Purif Technol* 117:18–23. <https://doi.org/10.1016/j.seppur.2013.04.026>
53. Liu C, Wu B, Chen X, Xie S (2017) Waste activated sludge pretreatment by Fe(II)-activated peroxymonosulfate oxidation under mild temperature. *Chem Pap* 71(12):2343–2351. <https://doi.org/10.1007/s11696-017-0228-2>
54. Wu J, Zhang H, Qui J (2012) Degradation of Acid Orange 7 in aqueous solution by a novel electro/Fe²⁺/peroxydisulfate process. *J Hazard Mater* 215–216:138–145. <https://doi.org/10.1016/j.jhazmat.2012.02.047>
55. Crimi ML, Taylor J (2007) Experimental evaluation of catalyzed hydrogen peroxide and sodium persulfate for destruction of BTEX contaminants. *Soil Sediment Contam* 16:29–45. <https://doi.org/10.1080/15320380601077792>
56. Georgi A, Kopinke FD (2005) Interaction of adsorption and catalytic reactions in water decontamination processes. Part I. Oxidation of organic contaminants with hydrogen peroxide catalyzed by activated carbon. *Appl Catal B* 58:9–18. <https://doi.org/10.1016/j.apcatb.2004.11.014>
57. Kolthoff IM, Miller IK (1951) The chemistry of persulfate I. The kinetics and mechanism of the decomposition of the persulfate ion in aqueous medium. *J Am Chem Soc* 73:3055–3059. <https://doi.org/10.1021/ja01151a024>
58. Martinez-Huitle CA, Brillas E (2009) Decontamination of wastewater containing synthetic organic dyes by electrochemical methods: a general review. *Appl Catal B* 87:105–145. <https://doi.org/10.1016/j.apcatb.2008.09.017>
59. Barbosa J, Fernandes A, Ciriaco L, Lopes A, Pacheco MJ (2016) Electrochemical treatment of olive processing wastewater using a boron-doped diamond anode. *Clean Soil Air Water* 44:1242–1249. <https://doi.org/10.1002/clen.201500158>
60. Gotsi M, Kalogerakis N, Psillakis E, Samaras P, Mantzavinos D (2005) Electrochemical oxidation of olive oil mill wastewaters. *Water Res* 39:4177–4187. <https://doi.org/10.1016/j.watres.2005.07.037>
61. Belaid C, Khadraoui M, Mseddi S, Kallel M, Elleuch B, Fauvarque JF (2013) Electrochemical treatment of olive mill wastewater: treatment extent and effluent phenolic compounds monitoring using some uncommon analytical tools. *J Environ Sci* 25:220–230. [https://doi.org/10.1016/S1001-0742\(12\)60037-0](https://doi.org/10.1016/S1001-0742(12)60037-0)
62. Deligiorgis A, Xekoukoulotakis NP, Diamadopoulos E, Mantzavinos D (2008) Electrochemical oxidation of table olive processing wastewater over boron-doped diamond electrodes: treatment optimization by factorial design. *Water Res* 42:1229–1237. <https://doi.org/10.1016/j.watres.2007.09.014>
63. Giannis A, Kalaitzakis M, Diamadopoulos E (2007) Electrochemical treatment of olive mill wastewater. *J Chem Technol Biotechnol* 82:663–671. <https://doi.org/10.1002/jctb.1725>
64. Bellekhal N, Oturan MA, Oturan N, Dachraoui M (2006) Olive oil mill wastewater treatment by electro-Fenton process. *Environ Chem* 3:345–349. <https://doi.org/10.1071/EN05080>
65. Panizza M, Cerisola G (2006) Olive mill wastewater treatment by anodic oxidation with parallel plate electrodes. *Water Res* 40:1179–1184. <https://doi.org/10.1016/j.watres.2006.01.020>

Publisher's Note Springer Nature remains neutral with regard to jurisdictional claims in published maps and institutional affiliations.